Locking-free finite element methods for linear and nonlinear elasticity in 2D and 3D ⋆

K.S. Chavan, B.P. Lamichhane *, B.I. Wohlmuth

Universität Stuttgart, Institut für Angewandte Analysis und Numerische Simulation, Pfaffenwaldring 57, D-70569 Stuttgart, Germany

Abstract

The uniform convergence of finite element approximations based on a modified Hu-Washizu formulation for the nearly incompressible linear elasticity is analyzed. We show the optimal and robust convergence of the displacement-based discrete formulation in the nearly incompressible case with the choice of approximations based on quadrilateral and hexahedral elements. These choices include bases that are well known, as well as newly constructed bases. Starting from a suitable three-field problem, we extend our α-dependent three-field formulation to geometrically nonlinear elasticity with Saint-Venant Kirchhoff law. Additionally, an α-dependent three-field formulation for a general hyperelastic material model is proposed. A range of numerical examples using different material laws for small and large strain elasticity is presented.

Key words: Hu-Washizu formulation, mixed finite elements, low-order approximations, uniform convergence

1 Introduction

It is well-known that standard low-order finite elements based on four-noded quadrilaterals or eight-noded hexahedra have two drawbacks in finite element computation. The first one is the locking effect in the nearly incompressible case; in other words, they do not converge uniformly with respect to the Lamé parameter λ. The second one is that these standard elements lead to poor accuracy in bending-dominated problems when coarse meshes are used. There are

⋆ Supported in part by the Deutsche Forschungsgemeinschaft, SFB 404, B8.

* Corresponding author.
Email address: blamichha@yahoo.com (B.P. Lamichhane).

many approaches to overcome these difficulties. Among them are the methods associated with the enhancement of the strain or stress field. The method of enhanced assumed strain, first proposed by Simo and Rifai [1], has become a popular approach; see, e.g., [2–4]. A detailed mathematical analysis of enhanced assumed strain has been done by Braess, Carstensen and Reddy [5], where a robust asymptotic convergence of the error in the displacement has been proved for a class of meshes. The assumed stress approach proposed in [6] has a very similar feature to that based on enhanced strains, and in fact the two methods are equivalent under some assumptions on the discrete spaces [7,5]. Simo and Rifai have started from the Hu–Washizu principle [8,9] to derive a method based on the enhancement of the strains. We note that this idea has been also successfully extended to the nonlinear setting. A different idea using the Hu–Washihzu formulation as starting point results in the mixed enhanced strain approach introduced by Kasper and Taylor [10]. Static condensation of the stress and strain yields a displacement based formulation. The method of the mixed enhanced strain is also applied to nonlinear hyperelasticity [11]. Another relevant approach having a close link with the Hu–Washizu formulation is the strain gap method due to Romano, Marotti, and Diaco [12]. However, the analysis presented in [12] does not cover the uniform convergence of the finite element solution in the nearly incompressible case. All these methods, variationally based on the Hu–Washizu principle, yield a promising approach to overcome the difficulties referred to earlier. However, there were open questions on the full mathematical analysis of the Hu–Washizu formulation. This gap has been filled by a recent work on the uniform convergence of the Hu–Washizu formulation in the nearly incompressible case, see [13]. The uniform convergence of the finite element solution in the nearly incompressible case has been shown through a parameter dependent modification that is equivalent to the standard Hu–Washizu formulation in the continuous setting. However, in the discrete setting the new modified Hu–Washizu formulation results in a possibly parameter dependent finite element solution

The essential point of the analysis in [13] is the requirement that the discrete space of displacements V_h forms, with the trace space of a discrete spherical part of S_h, a Stokes-stable pair, i.e. a uniform inf-sup condition with a constant independent of h and λ is satisfied. We note that in the discrete setting, the spherical part of the stress field is not necessarily in the discrete space of stresses. Thus we use a orthogonal decomposition and a suitable projection operator to define a discrete spherical part which is a subspace of the discrete space for the stresses. If bilinear or trilinear elements are used to discretize the displacement field this condition is, in general, not satisfied, so that spurious modes might be present. However it can be shown that the discretization error of the displacement is not affected by these spurious modes.

In this paper, we extend the analysis of [13] to the three-dimensional lin-

ear elasticity and consider also the nonlinear case. We present the spaces of stresses and strains which satisfy the conditions of well-posedness for linear elasticity in three dimensions. Moreover, we extend our formulation to geometrically nonlinear elasticity with Saint-Venant Kirchhoff law. Furthermore, an α-dependent three-field formulation for a general hyperelastic model is proposed. We note that the presented mathematical analysis is restricted to the linear case. Finally, we illustrate the numerical performance of all our formulations by considering different nonlinear material laws and small and large strain elasticity.

The structure of the rest of the paper is organized as follows. In the next section, we briefly recall the standard and the modified Hu–Washizu formulation of linear elasticity. In Section 3, we present examples of discrete spaces for the stress and strain which satisfy the conditions of well-posedness and which will be used in our numerical computations. Moreover, we summarize the results shown in [13] for the two-dimensional setting and extend them to the three-dimensional case. In Section 4, we consider the geometrically nonlinear situation with Saint-Venant Kirchhoff law. The idea of an α-dependent three-field formulation is generalized to hyperelastic material laws in Section 5. Finally, numerical results are presented in the last section.

2 The boundary value problem of linear elasticity

We assume that a bounded domain Ω in $\mathbb{R}^N$, $N = \{2, 3\}$, with piecewise Lipschitz boundary Γ is occupied by a homogeneous isotropic linear elastic material. Given a body force $\boldsymbol{f} \in L^2(\Omega)^N$, we consider the equilibrium equation in Ω

$$-\operatorname{div} \boldsymbol{\sigma} = \boldsymbol{f} \ , \tag{2.1}$$

where the symmetric Cauchy stress tensor $\boldsymbol{\sigma}$ is related to the strain tensor $\boldsymbol{d}$ by the Saint-Venant Kirchhoff constitutive relation written in terms of the elasticity tensor $\mathcal{C}$ as

$$\boldsymbol{\sigma} = \mathcal{C}\boldsymbol{d} := \lambda(\operatorname{tr} \boldsymbol{d})\mathbf{1} + 2\mu\, \boldsymbol{d} \ . \tag{2.2}$$

Here, $\mathbf{1}$ is the identity tensor; and λ and μ are the Lamé parameters, which are assumed to be constant and positive. We are interested in the case of incompressible limit, which corresponds to $\lambda \to \infty$. The infinitesimal strain tensor $\boldsymbol{d}$ is defined as a linear function of the displacement $\boldsymbol{u}$ by

$$\boldsymbol{d} = \boldsymbol{\varepsilon}(\boldsymbol{u}) := \tfrac{1}{2}(\nabla \boldsymbol{u} + [\nabla \boldsymbol{u}]^t) \ , \tag{2.3}$$

and, for simplicity, we assume homogeneous Dirichlet boundary condition for the displacement $\boldsymbol{u}$.

Introducing the Sobolev space $V := [H_0^1(\Omega)]^N$ of displacements with standard inner product $(\cdot,\cdot)_1$ and norm $\|\cdot\|_1$, we define the bilinear form $A(\cdot,\cdot)$ and the linear functional $\ell(\cdot)$ by

$$\begin{aligned} A : V \times V \to \mathbb{R}, \quad & A(\boldsymbol{u},\boldsymbol{v}) := \textstyle\int_\Omega \mathcal{C}\boldsymbol{\varepsilon}(\boldsymbol{u}) : \boldsymbol{\varepsilon}(\boldsymbol{v})\ dx\ , \\ \ell : V \to \mathbb{R}, \quad & \ell(\boldsymbol{v}) := \textstyle\int_\Omega \boldsymbol{f}\cdot\boldsymbol{v}\ dx\ . \end{aligned}$$

Then the standard weak form of the linear elasticity problem is as follows: given $\ell \in V'$, find $\boldsymbol{u} \in V$ that satisfies

$$A(\boldsymbol{u},\boldsymbol{v}) = \ell(\boldsymbol{v})\ , \quad \boldsymbol{v} \in V\ . \tag{2.4}$$

Since $A(\cdot,\cdot)$ is symmetric, continuous, and V-elliptic under the assumptions on $\mathcal{C}$, standard arguments can be used to show that (2.4) has a unique solution $\boldsymbol{u} \in V$. Furthermore, we assume that the domain Ω is convex and smooth enough such that $\boldsymbol{u} \in [H^2(\Omega)]^N \cap V$, and there exists a constant C independent of λ such that

$$\|\boldsymbol{u}\|_2 + \lambda \|\operatorname{div}\boldsymbol{u}\|_1 \le C\,\|\boldsymbol{f}\|_0\ . \tag{2.5}$$

The a priori estimate (2.5) has been shown in [14] for the two-dimensional linear elasticity posed in a convex domain with polygonal boundary, see also [15].

We also introduce the space of stresses S and the space of strains D, where $D := \{\boldsymbol{e} \mid e_{ji} = e_{ij},\ e_{ij} \in L^2(\Omega),\ 1 \le i,j \le N\} =: S$ with the norm $\|\cdot\|_0$ generated in the standard way by the L^2-norm. We also need the space S_0, which is a closed subspace of S defined by $S_0 := \{\boldsymbol{\tau} \in S \mid (\boldsymbol{\tau},\mathbf{1})_0 = 0\}$.

The standard Hu–Washizu formulation is obtained by considering the constitutive equation (2.2), the strain-displacement equation (2.3) and the equation of equilibrium (2.1) in a weak form. Although the existence and the uniqueness of the solution of the standard Hu–Washizu formulation can be shown, the continuity constant of one of the involved bilinear forms tends to infinity as λ does, and thus all a priori results depend in a sensitive way on λ. Therefore, we consider a modification of the Hu–Washizu formulation depending on a parameter $\alpha \in \mathbb{R}$: find $(\boldsymbol{u},\boldsymbol{d},\boldsymbol{\sigma}) \in V \times D \times S_0$ such that

$$\begin{aligned} a_\alpha((\boldsymbol{u},\boldsymbol{d}),(\boldsymbol{v},\boldsymbol{e})) + b_\alpha((\boldsymbol{v},\boldsymbol{e}),\boldsymbol{\sigma}) &= \ell(\boldsymbol{v})\ , \quad && (\boldsymbol{v},\boldsymbol{e}) \in V \times D\ , \\ b_\alpha((\boldsymbol{u},\boldsymbol{d}),\boldsymbol{\tau}) - \tfrac{\delta}{\kappa}\, c(\boldsymbol{\sigma},\boldsymbol{\tau}) &= 0\ , && \boldsymbol{\tau} \in S_0\ , \end{aligned} \tag{2.6}$$

where the bilinear forms are defined by

$$\begin{aligned} a_\alpha((\boldsymbol{u},\boldsymbol{d}),(\boldsymbol{v},\boldsymbol{e})) &:= 2\mu(\boldsymbol{d},\boldsymbol{e})_0 + \alpha\mu(\operatorname{tr}\boldsymbol{d},\operatorname{tr}\boldsymbol{e})_0\ , \\ b_\alpha((\boldsymbol{v},\boldsymbol{e}),\boldsymbol{\sigma}) &:= (\boldsymbol{\varepsilon}(\boldsymbol{v}) - \boldsymbol{e},\boldsymbol{\sigma})_0 + \delta(\operatorname{tr}\boldsymbol{\sigma},\operatorname{tr}\boldsymbol{e})_0\ , \\ c(\boldsymbol{\sigma},\boldsymbol{\tau}) &:= (\operatorname{tr}\boldsymbol{\sigma},\operatorname{tr}\boldsymbol{\tau})_0\ , \end{aligned}$$

and $\kappa := 2\mu + N\lambda$, $\delta := \frac{(\lambda - \alpha\mu)}{\kappa}$. The standard Hu–Washizu formulation can be obtained by setting $\alpha = \frac{\lambda}{\mu}$ in (2.6). We note that the solution of (2.6) does not depend on α. The existence of a unique solution has been established in [13].

3 Discrete formulations

Suppose that $\mathcal{T}_h$ is a quasi-uniform and shape-regular quadrilateral or hexahedral triangulation of the polygonal or polyhedral domain Ω. Each element $K \in \mathcal{T}_h$ is generated by an isoparametric map F_K from the reference element $\hat{K} := (-1, 1)^N$. We recall that if $\hat{v} \in \mathcal{Q}_1(\hat{K})$, $\mathcal{Q}_1(\hat{K})$ being the space of bilinear or trilinear polynomials on $\hat{K}$, then $\hat{v} \circ F_K^{-1}$ is in general not a polynomial on the quadrilateral or hexahedron K. However, for the theoretical analysis, we assume that F_K is an affine mapping for each element $K \in \mathcal{T}_h$. The finite element spaces for the displacement, stress and strain are defined as

$$V_h := \left\{ \boldsymbol{v}_h \in V,\ \boldsymbol{v}_h|_K = \hat{\boldsymbol{v}}_h \circ F_K^{-1}, \hat{\boldsymbol{v}}_h \in \mathcal{Q}_1(\hat{K})^N \ \text{ for all } \ K \in \mathcal{T}_h \right\} ,$$

$$S_h := \left\{ \boldsymbol{\tau}_h \in S_0 \mid (\boldsymbol{\tau}_h|_K)_{ij} = (\hat{\boldsymbol{\tau}}_h)_{ij} \circ F_K^{-1}, \ \ \hat{\boldsymbol{\tau}}_h \in S_\square \text{ for all } K \in \mathcal{T}_h \right\} ,$$

$$D_h := \left\{ \boldsymbol{e}_h \in S_0 \mid (\boldsymbol{e}_h|_K)_{ij} = (\hat{\boldsymbol{e}}_h)_{ij} \circ F_K^{-1}, \ \ \hat{\boldsymbol{e}}_h \in D_\square \text{ for all } K \in \mathcal{T}_h \right\} ,$$

respectively, where $D_\square$ and $S_\square$ are the reference bases of strains and stresses defined on $\hat{K}$. These two variables are defined locally on each element and no continuity condition applies at the element boundaries. In the following, we need additionally the space M_h defined by $M_h := \operatorname{tr} S_h$.

We recall the Voigt representation of the tensorial quantities stress and strain in vectorial form in two and three dimensions

$$\begin{aligned} \boldsymbol{\sigma} &= [\sigma_{11}, \sigma_{22}, \sigma_{12}]^T , \quad \boldsymbol{d} = [d_{11}, d_{22}, 2d_{12}]^T ; \quad \text{and} \\ \boldsymbol{\sigma} &= [\sigma_{11}, \sigma_{22}, \sigma_{33}, \sigma_{12}, \sigma_{23}, \sigma_{13}]^T , \quad \boldsymbol{d} = [d_{11}, d_{22}, d_{33}, 2d_{12}, 2d_{23}, 2d_{13}]^T , \end{aligned}$$

respectively. It is easy to see that this representation yields $\boldsymbol{\sigma}^T \boldsymbol{d} = \sum_{i,j} \sigma_{ij} d_{ij} = \boldsymbol{\sigma} : \boldsymbol{d}$, where on the left the scalar product is applied on the vectorial quantities and on the right the product is applied to the tensorial quantities. The spaces S_h and D_h will be generated from bases defined on $\hat{K}$, and we will make use of the following bases on $\hat{K}$:

$$A_2 := \text{span}\begin{bmatrix} \hat{y} & 0 \\ 0 & \hat{x} \\ 0 & 0 \end{bmatrix}, \qquad A_3 := \text{span}\begin{bmatrix} \hat{y} & \hat{z} & \hat{y}\hat{z} & 0 & 0 & 0 & 0 & 0 & 0 & 0 & 0 & 0 \\ 0 & 0 & 0 & \hat{x} & \hat{z} & \hat{x}\hat{z} & 0 & 0 & 0 & 0 & 0 & 0 \\ 0 & 0 & 0 & 0 & 0 & 0 & \hat{x} & \hat{y} & \hat{x}\hat{y} & 0 & 0 & 0 \\ 0 & 0 & 0 & 0 & 0 & 0 & 0 & 0 & 0 & \hat{z} & 0 & 0 \\ 0 & 0 & 0 & 0 & 0 & 0 & 0 & 0 & 0 & 0 & \hat{x} & 0 \\ 0 & 0 & 0 & 0 & 0 & 0 & 0 & 0 & 0 & 0 & 0 & \hat{y} \end{bmatrix},$$

$$B_2 := \text{span}\begin{bmatrix} \hat{x} & 0 \\ 0 & \hat{y} \\ 0 & 0 \end{bmatrix}, \qquad B_3 := \text{span}\begin{bmatrix} \hat{x} & \hat{x}\hat{y} & \hat{x}\hat{z} & 0 & 0 & 0 & 0 & 0 & 0 \\ 0 & 0 & 0 & \hat{y} & \hat{y}\hat{z} & \hat{x}\hat{y} & 0 & 0 & 0 \\ 0 & 0 & 0 & 0 & 0 & 0 & \hat{z} & \hat{y}\hat{z} & \hat{x}\hat{z} \\ 0 & 0 & 0 & 0 & 0 & 0 & 0 & 0 & 0 \\ 0 & 0 & 0 & 0 & 0 & 0 & 0 & 0 & 0 \\ 0 & 0 & 0 & 0 & 0 & 0 & 0 & 0 & 0 \end{bmatrix},$$

$$C_2 := \text{span}\begin{bmatrix} 0 & 0 \\ 0 & 0 \\ \hat{x} & \hat{y} \end{bmatrix}, \qquad C_3 := \text{span}\begin{bmatrix} 0 & 0 & 0 & 0 & 0 & 0 & 0 & 0 & 0 \\ 0 & 0 & 0 & 0 & 0 & 0 & 0 & 0 & 0 \\ 0 & 0 & 0 & 0 & 0 & 0 & 0 & 0 & 0 \\ \hat{x} & \hat{y} & \hat{z} & 0 & 0 & 0 & 0 & 0 & 0 \\ 0 & 0 & 0 & \hat{x} & \hat{y} & \hat{z} & 0 & 0 & 0 \\ 0 & 0 & 0 & 0 & 0 & 0 & \hat{x} & \hat{y} & \hat{z} \end{bmatrix},$$

$$D_2 := \text{span}\begin{bmatrix} 0 & 0 \\ 0 & 0 \\ \hat{x} & \hat{y} \end{bmatrix}, \qquad D_3 := \text{span}\begin{bmatrix} 0 & 0 & 0 & 0 & 0 & 0 & 0 & 0 & 0 & 0 & 0 & 0 \\ 0 & 0 & 0 & 0 & 0 & 0 & 0 & 0 & 0 & 0 & 0 & 0 \\ 0 & 0 & 0 & 0 & 0 & 0 & 0 & 0 & 0 & 0 & 0 & 0 \\ \hat{x} & \hat{y} & \hat{y}\hat{z} & \hat{x}\hat{z} & 0 & 0 & 0 & 0 & 0 & 0 & 0 & 0 \\ 0 & 0 & 0 & 0 & \hat{y} & \hat{z} & \hat{x}\hat{z} & \hat{x}\hat{y} & 0 & 0 & 0 & 0 \\ 0 & 0 & 0 & 0 & 0 & 0 & 0 & \hat{z} & \hat{x} & \hat{x}\hat{y} & \hat{y}\hat{z} \end{bmatrix},$$

where the lower index 2 or 3 stands for the space dimension. We note that $C_2 = D_2$ but $C_3 \neq D_3$. Of special interest will be the choices (S_h^i, D_h^i), $1 \leq i \leq 5$ given in Table 1. Here, $\mathcal{I}_N$ stands for the span of the identity tensor in N dimensions and is of dimension one. We note that the five different spaces

Table 1
Different cases for the discrete spaces, $N = 2, 3$

Case	I	II	III	IV	V
$S_\square$	$\mathcal{I}_N + A_N$	$\mathcal{I}_N + A_N$	$\mathcal{I}_N + C_N$	$\mathcal{I}_N + A_N + D_N$	$\mathcal{I}_N + A_N + D_N$
$D_\square$	$\mathcal{I}_N + A_N$	$\mathcal{I}_N + A_N + B_N$	$\mathcal{I}_N + C_N$	$\mathcal{I}_N + A_N + D_N$	$\mathcal{I}_N + A_N + B_N + D_N$
	$S_h^1 = D_h^1$	$S_h^2 \subset D_h^2$	$S_h^3 = D_h^3$	$S_h^4 = D_h^4$	$S_h^5 \subset D_h^5$

of stresses and strains have been considered for the two-dimensional setting in [13], and here we introduce the associated three dimensional cases. The spaces of stresses and strains for both dimensions can simply be obtained from Table 1 by setting $N = 2$ or $N = 3$. Case II corresponds to the method of mixed enhanced strains [10,11] while Case V corresponds to the method of enhanced assumed strains [1]. The Cases IV and V are in three dimensions more involved because in contrast to the two-dimensional situation, we cannot work with C_3 but have to introduce the new space D_3.

The discrete α-dependent Hu–Washizu formulation is as follows: find $(\boldsymbol{u}_h^\alpha, \boldsymbol{d}_h^\alpha, \boldsymbol{\sigma}_h^\alpha) \in V_h \times D_h \times S_h$ such that

$$\begin{aligned} a_\alpha((\boldsymbol{u}_h^\alpha, \boldsymbol{d}_h^\alpha), (\boldsymbol{v}_h, \boldsymbol{e}_h)) + b_\alpha((\boldsymbol{v}_h, \boldsymbol{e}_h), \boldsymbol{\sigma}_h^\alpha) &= \ell(\boldsymbol{v}_h), \ (\boldsymbol{v}_h, \boldsymbol{e}_h) \in V_h \times D_h \ , \\ b_\alpha((\boldsymbol{u}_h^\alpha, \boldsymbol{d}_h^\alpha), \boldsymbol{\tau}_h) \qquad - \tfrac{\delta}{\kappa}\, c(\boldsymbol{\sigma}_h^\alpha, \boldsymbol{\tau}_h) \qquad &= \quad 0, \qquad\qquad \boldsymbol{\tau}_h \in S_h \ . \end{aligned} \tag{3.1}$$

Although the continuous solution of (2.6) is independent of α, the discrete solution can depend on α. However, for simplicity of notation from now on we replace $(\boldsymbol{u}_h^\alpha, \boldsymbol{d}_h^\alpha, \boldsymbol{\sigma}_h^\alpha)$ by $(\boldsymbol{u}_h, \boldsymbol{d}_h, \boldsymbol{\sigma}_h)$.

In the following, we assume that $S_h \subset D_h$, and we restrict ourselves to two types of discretization.

- Type 1: $S_h \subset D_h$ and $\operatorname{tr} D_h \mathbf{1} \subset D_h$.
- Type 2: $S_h = D_h$ and $\operatorname{tr} D_h \mathbf{1} \not\subset D_h$.

For discretizations of Type 1, the numerical solution does not depend on $\alpha \neq -1$, whereas for the discretizations of Type 2, it depends on α, see also the numerical results of Section 6 and the theoretical result of [13]. We note that the Cases II, III and V in Table 1 correspond to a discretization of Type 1, and the Cases I and IV correspond to one of Type 2. Case IV for $\alpha = \frac{\lambda}{\mu}$ is equivalent to the standard Q_1-approach and thus yields poor numerical results in the nearly incompressible limit. The link between the modified Hu–Washizu formulation (3.1), the Hellinger–Reissner, Mixed Enhanced Strain, Enhanced Assumed Strain and the classical Q_1-P_0 formulation has been discussed in detail in [16].

The rest of this section is devoted to summarizing some relevant results proved in [13] for the modified Hu–Washizu formulation in planar elasticity, which can

easily be extended to the three-dimensional case. Since the spherical part of the stress plays a crucial role in the analysis of the incompressible limit, we define the L^2-orthogonal projections sph and dev on S by $\operatorname{sph}\boldsymbol{\tau} := \frac{1}{N}(\operatorname{tr}\boldsymbol{\tau})\mathbf{1}$, and $\operatorname{dev}\boldsymbol{\tau} := \boldsymbol{\tau} - \operatorname{sph}\boldsymbol{\tau}$. In contrast to the continuous setting, $\operatorname{dev} S_h$ and $\operatorname{sph} S_h$ are in general not subspaces of S_h, and therefore, we introduce the discrete deviatoric operator $\operatorname{dev_h}$ defined by $\operatorname{dev_h} S_h := P_{S_h} \operatorname{dev} S_h$, where P_{S_h} is the L^2-orthogonal projection onto S_h, and decompose S_h according to

$$S_h = \operatorname{dev_h} S_h \oplus \operatorname{sph_h} S_h \,. \tag{3.2}$$

Next, we define $\widetilde{M}_h := \operatorname{tr}\operatorname{sph_h} S_h$, and find that $\widetilde{M}_h = \{q \in L^2_0(\Omega) \mid \ q|_K \in P_0(K),\ K \in \mathcal{T}_h\} \subset M_h$ for all our cases.

The analysis of the saddle point problem (3.1) is done in [13] for plane elasticity but can be quite easily extended to the three-dimensional case, see also [17,5]. The implementation of the modified Hu–Washizu formulation does not use the saddle point formulation (3.1) but is based on the positive definite displacement based system. Element-wise static condensation of the stress and the strain yields a symmetric and positive-definite system for the displacement

$$A_h(\boldsymbol{u}_h, \boldsymbol{v}_h) = \ell(\boldsymbol{v}_h)\,, \quad \boldsymbol{v}_h \in V_h \ . \tag{3.3}$$

To obtain the explicit expression for the discrete bilinear form $A_h(\boldsymbol{u}_h, \boldsymbol{v}_h)$, we decompose S_h orthogonally in $S_h = S_h^c \oplus S_h^t$ with $S_h^c := \{\boldsymbol{\tau} \in S_h \mid \ \mathcal{C}\boldsymbol{\tau} \in S_h\}$. We note that $S_h^t \subset \operatorname{dev_h} S_h$, $\operatorname{sph_h} S_h \subset S_h^c$ and $\operatorname{tr}(\operatorname{sph_h} S_h) = \operatorname{tr} S_h^c$. In the following, we provide two lemmas for $N \in \{2, 3\}$. These results can be found in [13] for $N = 2$, and the proof can easily be generalized to the case $N = 3$.

Lemma 1 *We define a scalar quantity $\theta(\mu, \lambda, \alpha)$ depending on the material parameters μ and λ and the stability parameter $\alpha \neq 1$. For the Cases II, III, V it is given by*

$$\theta(\mu, \lambda, \alpha) := \frac{2\mu(2\mu + N\lambda)}{2\mu + \lambda(N-1)} \ \textit{and by}$$
$$\theta(\mu, \lambda, \alpha) := \frac{(2\mu + N\lambda)^2 \mu(2+\alpha)}{\mu(2+\alpha)(2\mu + 2N\lambda - \lambda) + (N-1)^2\lambda^2} \ , \ \alpha \neq -2 \ ,$$

for the Cases I and IV. Then the bilinear form $A_h(\boldsymbol{u}_h, \boldsymbol{v}_h)$ is equal to:

$$A_h(\boldsymbol{u}_h, \boldsymbol{v}_h) = (Q_h\boldsymbol{\varepsilon}(\boldsymbol{u}_h), \boldsymbol{\varepsilon}(\boldsymbol{v}_h))_0 \ ,$$

where $Q_h\boldsymbol{\varepsilon}(\boldsymbol{u}_h) := \mathcal{C}P_{S_h^c}\boldsymbol{\varepsilon}(\boldsymbol{u}_h) + \theta(\mu, \lambda, \alpha)P_{S_h^t}\boldsymbol{\varepsilon}(\boldsymbol{u}_h)$, and $P_{S_h^c}$ and $P_{S_h^t}$ are orthogonal projections onto the spaces S_h^c and S_h^t, respectively.

The definition of the bilinear form $A_h(\cdot, \cdot)$ shows that it is symmetric and positive semi-definite. From this representation it follows directly that the

parameter α does not enter into the formulation for the Cases II, III, and V. Moreover, it is easy to see that $\theta(\mu, \lambda, \alpha)$ is uniformly bounded with respect to λ in the Cases I and IV if α is bounded uniformly. The classical Hu–Washizu formulation is given by $\alpha = \lambda/\mu$ and thus $\theta(\mu, \lambda, \alpha)$ grows linearly with respect to λ for the Cases I and IV.

We assume that the triangulation has a macro-structure so that $\widetilde{M}_{2h} \subset \widetilde{M}_h$, where $\widetilde{M}_{2h} := \{q \in L^2_0(\Omega) |\ q_{|K} \in P_0(K),\ K \in \mathcal{T}_{2h}\}$. Then the following theorem holds for all our cases.

Theorem 2 *For the Cases I and IV, we assume that α satisfies $0 < c_1 \leq \mu(2+\alpha) \leq C_1 < \infty$. Then under the regularity assumption (2.5), we obtain an optimal a priori estimate for the discretization error*

$$\|\boldsymbol{u} - \boldsymbol{u}_h\|_1 \leq Ch\|\boldsymbol{f}\|_0 \ ,$$

where $C < \infty$ is independent of λ and h.

Remark 3 *The results of Lemma 1 and Theorem 2 can be extended to other discretizations of Type 1 or Type 2. Suitable new pair of spaces (D_h, S_h) can be constructed by using the assumptions specified in [13]. A more detailed analysis shows that negative values of α might be also of interest. This is also reflected by our numerical results.*

4 Nonlinear elasticity with Saint-Venant Kirchhoff law

In this section, we extend our modified Hu–Washizu formulation to geometrically nonlinear elasticity with Saint-Venant Kirchhoff law. The three-field formulation for geometrically nonlinear elasticity with Saint-Venant Kirchhoff law is obtained by taking the symmetric second Piola–Kirchhoff stress, the Green–Lagrange strain and the displacement as unknowns. In a variational form, this consists of finding $(\boldsymbol{u}_h, \boldsymbol{d}_h, \boldsymbol{\sigma}_h) \in V_h \times D_h \times S_h$ that satisfy

$$\begin{aligned}
&\int_\Omega (\mathcal{C}\boldsymbol{d}_h - \boldsymbol{\sigma}_h) : \boldsymbol{e}_h \, dx &&= 0 \ , && \boldsymbol{e}_h \in D_h \ , \\
&\int_\Omega (\boldsymbol{E}(\boldsymbol{u}_h) - \boldsymbol{d}_h) : \boldsymbol{\tau}_h \, dx &&= 0 \ , && \boldsymbol{\tau}_h \in S_h \ , \\
&\int_\Omega (\mathbf{1} + \nabla \boldsymbol{u}_h)\boldsymbol{\sigma}_h : \nabla \boldsymbol{v}_h \, dx &&= \ell(\boldsymbol{v}_h) \ , && \boldsymbol{v}_h \in V_h \ ,
\end{aligned} \tag{4.1}$$

where D_h and S_h are as defined before, and $\boldsymbol{E}(\boldsymbol{u}_h) := \frac{1}{2}[(\mathbf{1} + \nabla \boldsymbol{u}_h)^T(\mathbf{1} + \nabla \boldsymbol{u}_h) - \mathbf{1}]$, $V_h \subset W^{1,4}(\Omega)^N$. The Sobolev space $W^{1,r}(\Omega)$ for $r \in \mathbb{N}$ is a Banach space and is defined in a standard way [18],

$$W^{1,r}(\Omega) := \{v \in L^1_{loc}(\Omega) : \|v\|^r_{0,\Omega} + \sum_{k=1}^{N} \|\frac{\partial v}{\partial x_k}\|^r_{L^r(\Omega)} < \infty\}$$

with $L^1_{loc}(\Omega)$ denoting the space of locally integrable functions in Ω. Working with this three-field formulation, we cannot expect that we obtain the uniform convergence of the numerical solution with respect to the Lamé parameter λ. As in the linear case, we can infer that the continuity constant of the form $(\mathcal{C}\boldsymbol{d}_h - \boldsymbol{\sigma}_h, \boldsymbol{e}_h)_0 = 0$ is not bounded independently of λ. Therefore, we introduce an α-dependent three-field formulation written as a nonlinear saddle point problem: find $(\boldsymbol{u}_h, \boldsymbol{d}_h, \boldsymbol{\sigma}_h) \in V_h \times D_h \times S_h$ such that

$$\begin{aligned} a_\alpha((\boldsymbol{u}_h, \boldsymbol{d}_h), (\boldsymbol{v}_h, \boldsymbol{e}_h)) + b^1_\alpha(\boldsymbol{u}_h, (\boldsymbol{v}_h, \boldsymbol{e}_h), \boldsymbol{\sigma}_h) &= \ell(\boldsymbol{v}_h) \ , \ (\boldsymbol{v}_h, \boldsymbol{e}_h) \in V_h \times D_h \ , \\ b^2_\alpha((\boldsymbol{u}_h, \boldsymbol{d}_h), \boldsymbol{\tau}_h) \quad - \quad \tfrac{\delta}{\kappa}\, c(\boldsymbol{\sigma}_h, \boldsymbol{\tau}_h) \quad &= \quad 0 \ , \qquad \boldsymbol{\tau}_h \in S_h \ , \end{aligned}$$

where the bilinear forms $a_\alpha(\cdot,\cdot)$ and $c(\cdot,\cdot)$, are defined as before, and

$$\begin{aligned} b^1_\alpha(\boldsymbol{u}, (\boldsymbol{v}, \boldsymbol{e}), \boldsymbol{\sigma}) &:= (\delta \operatorname{tr} \boldsymbol{\sigma} \mathbf{1} - \boldsymbol{\sigma}, \boldsymbol{e})_0 + ((\mathbf{1} + \nabla \boldsymbol{u})\boldsymbol{\sigma}, \nabla \boldsymbol{v})_0 \ , \\ b^2_\alpha((\boldsymbol{u}, \boldsymbol{d}), \boldsymbol{\tau}) &:= (\boldsymbol{E}(\boldsymbol{u}) - \boldsymbol{d}, \boldsymbol{\tau})_0 + \delta(\operatorname{tr} \boldsymbol{d}, \operatorname{tr} \boldsymbol{\tau})_0 \ . \end{aligned}$$

We note that if we replace $\boldsymbol{E}(\boldsymbol{u})$ by $\boldsymbol{\varepsilon}(\boldsymbol{u})$ in the definition of $b^2_\alpha(\cdot,\cdot)$, we find $b_\alpha(\cdot,\cdot)$, and if we replace $\mathbf{1} + \nabla \boldsymbol{u}$ by $\mathbf{1}$ in the definition of $b^1_\alpha(\cdot,\cdot)$, we find $b_\alpha(\cdot,\cdot)$. As in the case of linear elasticity, the solution of (4.2) does not depend on α under the assumption $\operatorname{tr} D_h \mathbf{1} \subset D_h$.

We recall a result concerning the equivalence between the Hu–Washizu and the Hellinger–Reissner formulation in the linear case. Stolarski and Belytschko [19] have shown that, if the spaces of stresses and strains satisfy the inclusion

$$S_h \subset \mathcal{C} D_h \ , \tag{4.2}$$

then the classical Hu–Washizu formulation is equivalent to the Hellinger–Reissner problem of finding $(\boldsymbol{u}_h, \boldsymbol{\sigma}_h) \in V_h \times S_h$ such that

$$\begin{aligned} \textstyle\int_\Omega \mathcal{C}^{-1}\boldsymbol{\sigma}_h : \boldsymbol{\tau}_h \, dx - \int_\Omega \boldsymbol{\varepsilon}(\boldsymbol{u}_h) : \boldsymbol{\tau}_h \, dx &= \quad 0 \ , \quad \boldsymbol{\tau}_h \in S_h \ , \\ \textstyle\int_\Omega \boldsymbol{\varepsilon}(\boldsymbol{v}_h) : \boldsymbol{\sigma}_h \, dx &= \ell(\boldsymbol{v}_h) \ , \ \boldsymbol{v}_h \in V_h \ . \end{aligned} \tag{4.3}$$

Under the assumption $\operatorname{tr} D_h \mathbf{1} \subset D_h$, the modified Hu–Washizu formulation (3.1) can be shown to be equivalent to the Hellinger–Reissner formulation (4.3), see [16].

As in the linear case, if $\operatorname{tr} D_h \mathbf{1} \subset D_h$, the geometrically nonlinear Hu–Washizu formulation (4.1) can be reduced to a two-field variational problem of Hellinger–Reissner type so that the weak discrete form can be written as: find $(\boldsymbol{u}_h, \boldsymbol{\sigma}_h) \in V_h \times S_h$ such that

$$\begin{aligned} \textstyle\int_\Omega \mathcal{C}^{-1}\boldsymbol{\sigma}_h : \boldsymbol{\tau}_h \, dx - \int_\Omega \boldsymbol{E}(\boldsymbol{u}_h) : \boldsymbol{\tau}_h \, dx &= \quad 0 \ , \quad \boldsymbol{\tau}_h \in S_h \ , \\ \textstyle\int_\Omega (\mathbf{1} + \nabla \boldsymbol{u}_h)\boldsymbol{\sigma}_h : \nabla \boldsymbol{v}_h \, dx &= \ell(\boldsymbol{v}_h) \ , \ \boldsymbol{v}_h \in V_h \ . \end{aligned} \tag{4.4}$$

Following exactly as in Lemma 1, the stress and strain can be statically condensed out from the system to obtain the following displacement-based formulation.

Lemma 4 *Defining $\theta(\cdot,\cdot,\cdot)$ and Q_h as in Lemma 1, the displacement-based formulation of* (4.2) *is given by*

$$((\mathbf{1}+\nabla \boldsymbol{u}_h)Q_h\boldsymbol{E}(\boldsymbol{u}_h),\nabla \boldsymbol{v}_h)_0=\ell(\boldsymbol{v}_h)$$

for all our cases.

5 Extension to general hyperelasticity

Using the inverse of the elasticity tensor $\mathcal{C}$, we have obtained an α-dependent three-field formulations for linear and geometrically nonlinear elasticity. In contrast to the linear Saint-Venant Kirchhoff law, the general hyperelastic constitutive equation cannot be inverted easily. As a consequence, we have to use a different starting point for the construction of our new α-dependent three-field formulation.

Under the assumption that the material is hyperelastic and isotropic a stored energy function W exists with $\boldsymbol{\sigma} = 2\frac{\partial W(\boldsymbol{C})}{\partial \boldsymbol{C}}$, where $\boldsymbol{\sigma}$ is the second Piola–Krichhoff stress tensor, and $\boldsymbol{C}$ is the right Cauchy–Green strain tensor given by $\boldsymbol{C} = \boldsymbol{F}^T\boldsymbol{F}$. The first Piola–Kirchhoff tensor $\boldsymbol{\pi}$ is related to the second Piola–Kirchhoff tensor $\boldsymbol{\sigma}$ by $\boldsymbol{\pi} = \boldsymbol{F}\boldsymbol{\sigma}$. Defining $\tilde{W}(\boldsymbol{F}) := W(\boldsymbol{C})$, we can write $\boldsymbol{\pi} = \frac{\partial \tilde{W}(\boldsymbol{F})}{\partial \boldsymbol{F}}$. For the isotropic material the energy function W depends only on the three principal invariants I_C, II_C and III_C of $\boldsymbol{C}$, where $I_C = \mathrm{tr}(\boldsymbol{C}), II_C = \frac{1}{2}(\mathrm{tr}^2(\boldsymbol{C}) - \mathrm{tr}(\boldsymbol{C}^2))$, and $III_C = \det(\boldsymbol{C}) = J^2$ with $J := \det(\boldsymbol{F})$. If the material law satisfies the two-term Mooney–Rivlin law [20], we have

$$\begin{aligned} W(\boldsymbol{C}) &= \lambda\, U(J) + \tfrac{\mu}{2}\left[(1-c_m)\,(I_C - 3 - 2\ln(J)) + c_m\,(II_C - 3 - 2\ln(J))\right] \,, \\ \boldsymbol{\sigma} &= \lambda U'(J) J\boldsymbol{C}^{-1} + \mu\left[(1-c_m)\left(\mathbf{1} - \boldsymbol{C}^{-1}\right) + c_m\left(\mathrm{tr}\,\boldsymbol{C}\mathbf{1} - \boldsymbol{C} - \boldsymbol{C}^{-1}\right)\right] \,, \end{aligned}$$

where c_m is a material constant. The real-valued function U is given by $U(J) = \frac{1}{4}(J^2 - 1 - 2\ln J)$. We recall that the standard neo-Hookean law is recovered with $c_m = 0$.

In the nonlinear Hu–Washizu formulation considered in [1,10,11], the displacement $\boldsymbol{u}$, the first Piola–Kirchhoff stress tensor $\boldsymbol{\pi}$ and the deformation gradient $\boldsymbol{F}$ are regarded as independent variables. Different Hu–Washizu functionals are considered in [21,22]. We start with the three-field formulation where the displacement $\boldsymbol{u}$, the Kirchhoff stress $\boldsymbol{\tau}$ and the deformation gradient $\boldsymbol{F}$ are

unknowns. We note that the Kirchhoff stress $\boldsymbol{\tau}$ is related to the second Piola–Kirchhoff stress $\boldsymbol{\sigma}$ by $\boldsymbol{\tau} = \boldsymbol{F}\boldsymbol{\sigma}\boldsymbol{F}^T$. Denoting the inverse of $\boldsymbol{F}^T$ by $\tilde{\boldsymbol{F}}$, this formulation in its strong form can be written as: given a body force $\mathbf{f} : \Omega \to \mathbb{R}^d$ and suitable boundary conditions on $\partial\Omega$, find $(\boldsymbol{u}, \boldsymbol{\tau}, \boldsymbol{F})$ such that

$$\begin{aligned} -\operatorname{div}(\boldsymbol{\tau}\tilde{\boldsymbol{F}}) &= \mathbf{f} \ , \\ \boldsymbol{\tau} &= \tfrac{\partial \tilde{W}(\boldsymbol{F})}{\partial \boldsymbol{F}} \boldsymbol{F}^T \ , \\ \boldsymbol{F} &= \mathbf{1} + \nabla \boldsymbol{u} \ . \end{aligned} \tag{5.1}$$

We point out that the first equation of (5.1) refers to the balance law, the second equation is the constitutive relation and the third one reflects the relation between the deformation gradient and the displacement field. We assume that the relation between the deformation gradient and the displacement is satisfied in the strong form and introduce

$$G(\boldsymbol{u}) := \frac{\partial \tilde{W}(\boldsymbol{F})}{\partial \boldsymbol{F}} \boldsymbol{F}^T \Big|_{\boldsymbol{F}=\mathbf{1}+\nabla \boldsymbol{u}}.$$

By doing so the three-field formulation can be reduced to a two-field formulation: find $(\boldsymbol{u}, \boldsymbol{\tau}) \in V \times S$ such that

$$\begin{aligned} \textstyle\int_\Omega \boldsymbol{\tau} : \nabla \boldsymbol{v} (\mathbf{1} + \nabla \boldsymbol{u})^{-1} \, dx &= \ell(\boldsymbol{v}) \ , \ \ \boldsymbol{v} \in V \ , \\ \textstyle\int_\Omega (\boldsymbol{\tau} - G(\boldsymbol{u})) : \boldsymbol{\zeta} \, dx &= 0 \ , \quad \boldsymbol{\zeta} \in S \ . \end{aligned}$$

Moreover, we decompose $G(\cdot)$ into $G(\boldsymbol{u}) = G_1(\boldsymbol{u}) + \lambda G_2(J)\mathbf{1}$. In the case of the Mooney–Rivlin material law, we can set $G_1(\boldsymbol{u}) = \mu(1 - c_m)\boldsymbol{B}(\boldsymbol{u}) + \mu c_m(\operatorname{tr} \boldsymbol{B}(\boldsymbol{u})\boldsymbol{B}(\boldsymbol{u}) - \boldsymbol{B}^2(\boldsymbol{u})) - \mu\mathbf{1}$ and $G_2(J) = U'(J)J$. Here $\boldsymbol{B}(\boldsymbol{u})$ is the left Cauchy–Green tensor defined by $\boldsymbol{B}(\boldsymbol{u}) := (\mathbf{1} + \nabla \boldsymbol{u})(\mathbf{1} + \nabla \boldsymbol{u})^T$. We note that $J \to 1$, $\lambda \to \infty$ and $G_2(J) \to 0$ for a nearly incompressible material.

To treat the nearly incompressible case, we introduce a pressure-like variable $p \in L^2(\Omega)$ and add the variational equation

$$\int_\Omega (p - \lambda G_2(J)) q \, dx = 0 \ , \ q \in L^2(\Omega) \ .$$

A similar pressure-like variable is introduced in [23] to study the convergence of finite element approximations of the nonlinear elasticity problems in the incompressible limit. Making use of the variable p, we define an α-dependent function $\tilde{G}(\boldsymbol{u}, p, \alpha) = G_1(\boldsymbol{u}) + \mu\alpha G_2(J)\mathbf{1} + (1 - \frac{\mu\alpha}{\lambda})p\mathbf{1}$ to arrive at an α-dependent three-field formulation involving the displacement $\boldsymbol{u}$, the Kirchhoff stress $\boldsymbol{\tau}$ and the pressure p. Combining all these three variational equations, our weak formulation reads: given a body force $\boldsymbol{f}$ and suitable boundary conditions on $\partial\Omega$ find $(\boldsymbol{u}, \boldsymbol{\tau}, p) \in V \times S \times L^2(\Omega)$ so that

$$
\begin{aligned}
\textstyle\int_\Omega \boldsymbol{\tau} : \nabla \boldsymbol{v} (\mathbf{1} + \nabla \boldsymbol{u})^{-1} \, dx &= \ell(\boldsymbol{v}) \ , \quad \boldsymbol{v} \in V \ , \\
\textstyle\int_\Omega (\boldsymbol{\tau} - \tilde{G}(\boldsymbol{u}, p, \alpha)) : \boldsymbol{\zeta} \, dx &= 0 \ , \quad \boldsymbol{\zeta} \in S \ , \\
\textstyle\int_\Omega (p - \lambda G_2(J)) q \, dx &= 0 \ , \quad q \in L^2(\Omega) \ ,
\end{aligned}
\tag{5.2}
$$

where $V \subset W^{1,r}(\Omega)$ with a suitable $r \geq 2$, see [24]. In the following, we concentrate on the three-field formulation (5.2). In contrast to the Hu–Washizu type formulation given in [11,2], we consider the symmetric Kirchhoff stress as an independent variable. Working with a symmetric tensor as unknown leads to a symmetric formulation and a reduction of the number of unknowns. Furthermore, we point out that the first and second Piola–Kirchhoff stress tensors are rational functions of the displacement and its gradient for the considered material laws, whereas the Kirchhoff stress depends polynomially on the displacement and its gradient. Since the stress will be discretized by using some piecewise polynomial space S_h, it is more reasonable to work with the Kirchhoff stress rather than first or second Piola–Kirchhoff stresses.

From the linear analysis, see also [13,5], it is crucial to project $G_2(J)$ onto piecewise constant functions to obtain a robust numerical scheme for the nearly incompressible case based on bilinear or trilinear finite element interpolations for the displacements. Therefore, the pressure is discretized by using piecewise constant functions, i.e., by $\widetilde{M}_h$, and the space of stress is discretized by defining a finite-dimensional space $S_\square$ on a reference element $\hat{K}$. Both stress and pressure variables are defined locally on each element and no continuity conditions apply at the element boundaries.

Defining the discrete determinant $J_h := \det(\mathbf{1} + \nabla \boldsymbol{u}_h)$ and using the discrete spaces introduced above, we can write our discrete three-field variational formulation as: find $(\boldsymbol{u}_h, \boldsymbol{\tau}_h, p_h) \in V_h \times S_h \times \widetilde{M}_h$ such that

$$
\begin{aligned}
\textstyle\int_\Omega \boldsymbol{\tau}_h : \nabla \boldsymbol{v}_h (\mathbf{1} + \nabla \boldsymbol{u}_h)^{-1} \, dx &= \ell(\boldsymbol{v}_h) \ , \quad \boldsymbol{v}_h \in V_h \ , \\
\textstyle\int_\Omega (\boldsymbol{\tau}_h - \tilde{G}(\boldsymbol{u}_h, p_h, \alpha)) : \boldsymbol{\zeta}_h \, dx &= 0 \ , \quad \boldsymbol{\zeta}_h \in S_h \ , \\
\textstyle\int_\Omega (p_h - \lambda G_2(J_h))) q_h \, dx &= 0 \ , \quad q_h \in \widetilde{M}_h \ .
\end{aligned}
\tag{5.3}
$$

We denote the projection onto the space of piecewise constant functions with respect to the mesh $\mathcal{T}_h$ by Π_h , Then, it is trivial to see that $p_h = \lambda \Pi_h G_2(J_h)$. Furthermore, static condensation of the stress from (5.3) yields the following displacement-based formulation.

Lemma 5 *The displacement-based formulation of* (5.3) *is given by*

$$
\int_\Omega P_{S_h} \tilde{G}(\boldsymbol{u}_h, p_h, \alpha) : \nabla \boldsymbol{v}_h (\mathbf{1} + \nabla \boldsymbol{u}_h)^{-1} \, dx = \ell(\boldsymbol{v}_h) \ ,
$$

where $p_h = \lambda \Pi_h G_2(J_h)$.

Lemma 6 *The numerical solution is independent of* α *if for* $\boldsymbol{\tau}_h \in S_h$*, the components of* $\boldsymbol{\tau}_h$ *restricted to an element of the mesh are constant.*

Proof. In this case, $P_{S_h}(G_2(J_h)\mathbf{1}) = \Pi_h G_2(J_h)\mathbf{1}$, and we have $P_{S_h}\tilde{G}(\boldsymbol{u}_h, p_h, \alpha) = P_{S_h}G(\boldsymbol{u}_h)$. The proof now follows by using the displacement-based formulation from Lemma 5. □

Although we have only the displacement and the stress as unknowns in our general nonlinear mixed formulation, we refer to the different cases by using the bases of the stress given in Table 1. We point out that since the spaces of stress are the same for Cases I and II, and for Cases IV and V, we have here only three distinct cases: Cases I, III and IV. Lemma 6 shows that the numerical solution is independent of α for Case III. We recall that for the Saint-Venant Kirchhoff law, we obtain also an α independent numerical solution not only for the Case III but also for the Cases II and V.

6 Numerical examples

In this section, we present some numerical examples in two and three dimensions using the bases of stresses and strains given in the previous sections. In particular, we show the locking-free response in the quasi-incompressible limit of the proposed formulation by comparing our results with the analytical solution and with the standard Q_1 finite element approach. The examples in two and three dimensions are based on four-noded quadrilateral elements with standard bilinear interpolation and eight-noded hexahedral elements with standard trilinear interpolation of the displacement field, respectively. We assume plane strain in the two-dimensional case. Our numerical results show an excellent performance of the proposed formulation in the nearly incompressible range whereas the standard case exhibits well-known volumetric locking. One example with a typical shear locking situation is also considered.

6.1 Example-I (Bending of a clamped plate)

In this classical numerical example [25] for a clamped plate subjected to bending, the formulation is tested for a bending dominated situation. A thin plate of dimension $2mm \times 2mm \times 0.01mm$ is considered. The plate is clamped along the complete boundary, and it is subjected to a uniformly distributed pressure of $-100\, N/mm^2$ on the top surface in z-direction [26]. A linear elastic material is considered with Young's modulus $E = 1.7472 \times 10^7 N/mm^2$ and Poisson's

ratio $\nu = 0.3$.

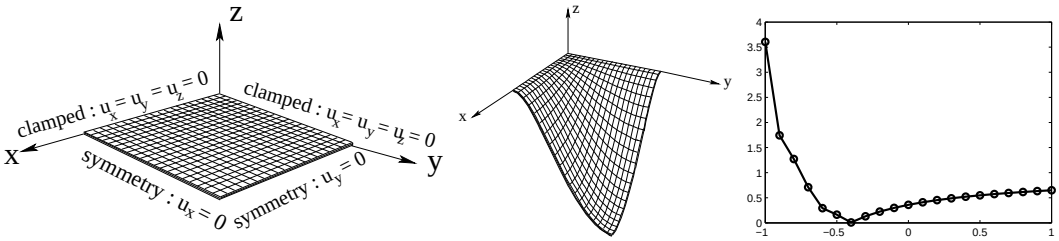

Fig. 1. Problem definition (left), deformed mesh (middle) and relative error versus $\frac{\alpha}{2}$ with Case I (right) (clamped plate)

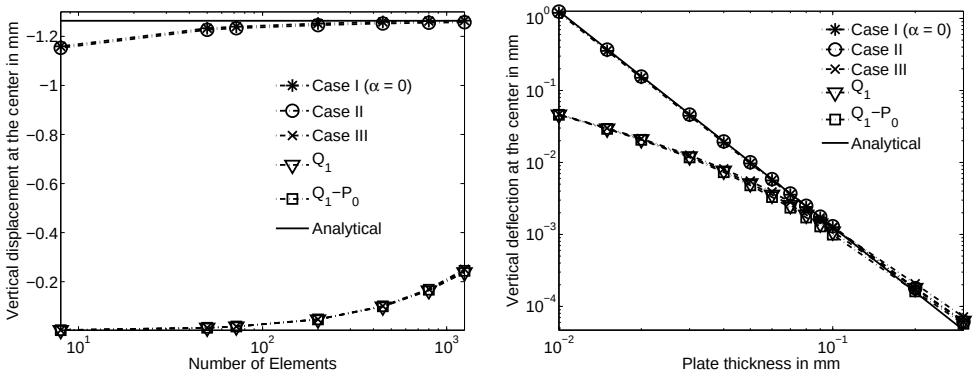

Fig. 2. Comparison of numerical results (clamped plate)

Taking advantage of the symmetry of the problem, only one fourth of the plate is discretized as shown in Figure 1, with two elements in z-direction. The convergence behavior of the proposed formulation with respect to the number of elements can be seen in the left picture of Figure 2. We find that Case II and Case I ($\alpha = 0$) yield extremely good coarse mesh accuracy, whereas Case III, Q_1 and Q_1-P_0 exhibit locking effect. In the right picture of Figure 2, the vertical deflection at the center of the plate with thickness ranging from $0.01mm$ to $0.3mm$ are compared with the analytical solution from Kirchhoff's plate theory. In this case, a finite element mesh with $10 \times 10 \times 2$ elements is used. We can see the increasing locking effect for Case III, Q_1 and Q_1-P_0 with decrease in thickness, whereas Case I ($\alpha = 0$) and Case II show extremely good results.

In a next step, we consider the nearly incompressible plate. The numerical solution at the center of the plate for Poisson's ratio $\nu = 0.4999$ is tabulated in Table 2. Case II works well whereas Case III gives similar results as Q_1-P_0 with shear locking and the standard Q_1 formulation gives results much worse than the other formulations. In the right picture of Figure 1, the relative error of the vertical deflection at the center of the plate ($\nu = 0.4999$) using Case I (mesh $10 \times 10 \times 2$) is plotted with respect to the parameter $\alpha/2$. Since we

do not have an exact solution for $\nu = 0.4999$, we compute the error using a reference solution from Case II with a very fine mesh. At $\alpha/2 \approx -0.4$, we find a minimum for the error. As α approaches -2 or $+2$, increasing locking effect can be observed.

Table 2
Vertical displacement at the center of the clamped plate

Number of Elements	Case I ($\alpha = 0$)	Case II	Case III	Q_1	Q_1-P_0
$25 \times 25 \times 2$	-0.7197	-1.0024	-0.2729	-0.0036	-0.2629
$20 \times 20 \times 2$	-0.7101	-0.9923	-0.18875	-0.0036	-0.1831
$15 \times 15 \times 2$	-0.6943	-0.9756	-0.1134	-0.0035	-0.1106
$10 \times 10 \times 2$	-0.6637	-0.9428	-0.05313	-0.0032	-0.0521
$6 \times 6 \times 2$	-0.6061	-0.8791	-0.0200	-0.0028	-0.0196
$5 \times 5 \times 2$	-0.5789	-0.8490	-0.0140	-0.0026	-0.0138
$2 \times 2 \times 2$	-0.2589	-0.4894	-0.0026	-0.0014	-0.0024

6.2 Example-II (Cook's membrane example)

In this popular benchmark example [1,10,27], we consider a two-dimensional tapered panel $\Omega := \text{conv}\{(0,0),(48,44),(48,60),(0,44)\}$, where $\text{conv}\{\xi\}$ represents the convex hull of the set ξ. The left boundary of the panel is clamped in both directions and the right boundary is subjected to an in-plane shear load in the positive y-direction as shown in the left picture of Figure 3. The material parameters $E = 250N/mm^2$ and $\nu = 0.4999$ are considered. Finite element analysis is performed using different discretizations with the initial mesh given in Figure 3. In the right picture of Figure 3, we show the relative error of the vertical displacement at T with respect to $\alpha/2$ using the mixed formulation (5.3) and the space of stress from Case I for neo-Hookean law after refining the initial mesh two times. The error is calculated using a reference solution from Case I with a very fine mesh. We observe that the locking increases with the increase in α.

In the left and the right pictures of Figure 4, we study the convergence of the numerical results with respect to the number of elements using different finite element formulations using Saint-Venant and neo-Hookean material model, respectively. We can see that for both material models all cases of the mixed formulation converge rapidly, whereas the standard displacement formulation shows the well-known locking effect. In particular, we observe a better coarse mesh accuracy from Cases II and III in the left picture of Figure 4, whereas Cases I and III give better results in coarse meshes in the right picture. We

recall that we have only three distinct cases (I, III and IV) for our mixed formulation with hyperelastic constitutive relation.

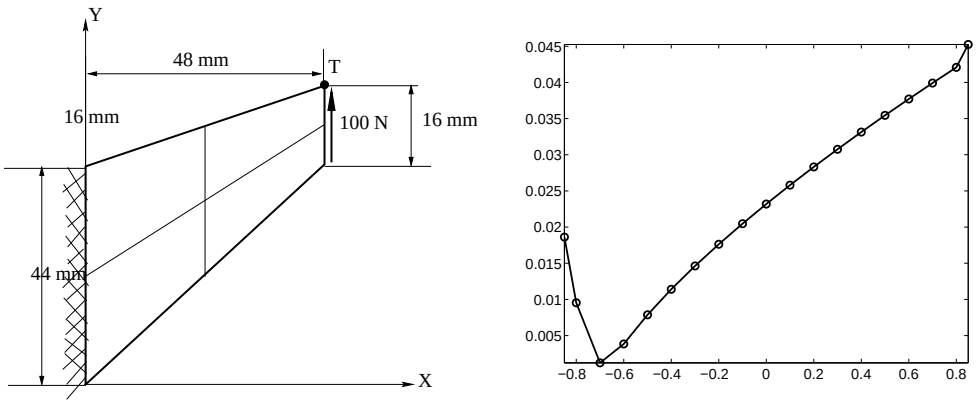

Fig. 3. Cook's membrane (geometrical data) and relative error in y-displacement at T versus $\frac{\alpha}{2}$ with neo-Hookean law

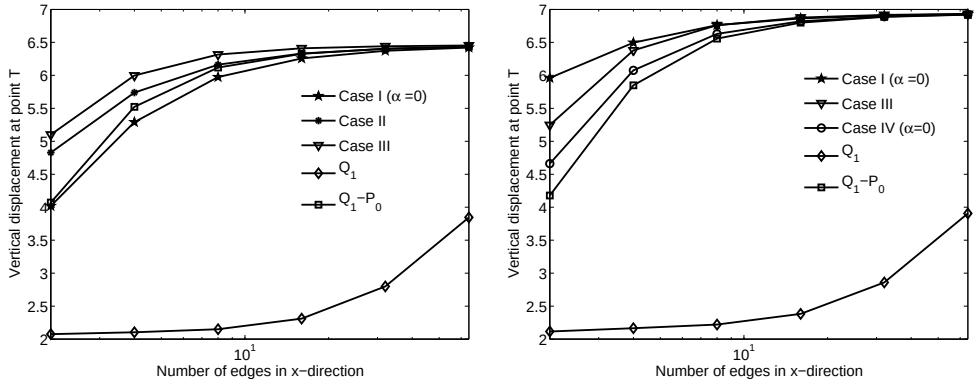

Fig. 4. Numerical results with Saint-Venant Kirchhoff material law (left) and neo-Hookean material law (right) (Cook's membrane)

6.3 Example-III (Arch subjected to bending load)

In this numerical example, the formulation is tested for bending condition. The fixed circular arch beam with $\theta_r = 60\ ^\circ$, $t = 0.1m$ and $r = 1m$ is considered as shown in Figure 5. The beam is subjected to a uniformly distributed load $P = 25N/m$ in radial direction on the upper boundary in a range of the angle θ_p=10°. Quasi-static finite element analysis is performed where the load is applied in incremental steps. The material parameters considered are $E = 250N/m^2$ and different values of Poisson's ratio ν as shown in Table 3.

In Table 3, the vertical deflection at the central point A is compared for the different formulations with Saint-Venant Kirchhoff material model with 5×80 finite element mesh in radial and angular directions. Similarly in Table 4, the

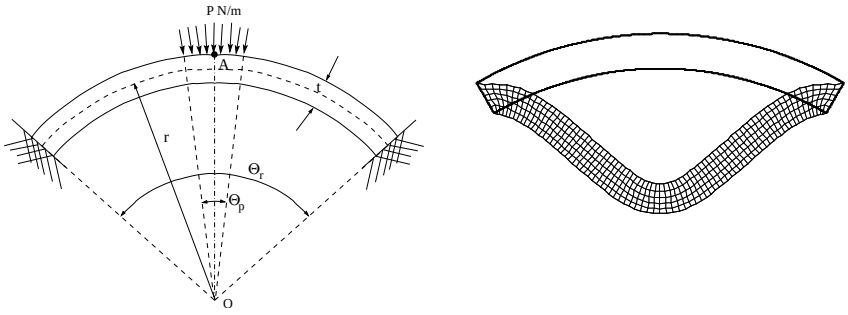

Fig. 5. Problem setting and deformed mesh (circular arch)

vertical deflection at the same point is compared for the different formulations using neo-Hookean material law. In both cases, the proposed mixed formulation shows better behavior while the standard Q_1 formulation shows locking as ν approaches 0.5. The deflected finite element mesh obtained for $\nu = 0.499$ using Case III of the mixed formulation with neo-Hookean material model is shown in the right picture of Figure 5. Load-deflection curves using the Saint-Venant Kirchhoff and the neo-Hookean material law for the Poisson's ratio $\nu = 0.499$ are compared in Figure 6. In both pictures, we can hardly see any difference among our different formulations.

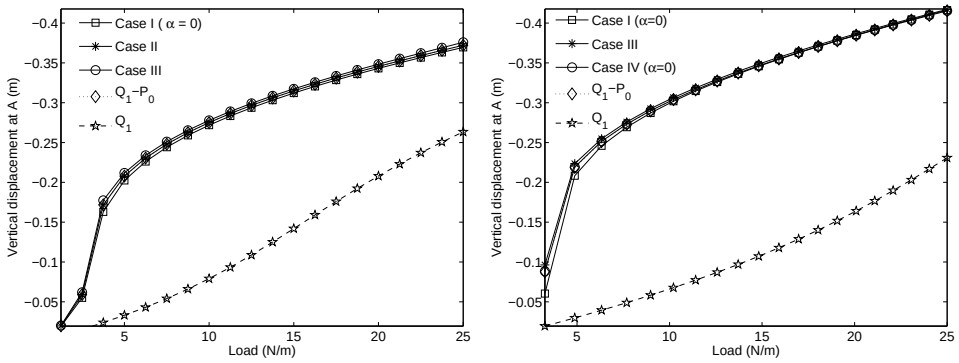

Fig. 6. Load-deflection curves for circular arch, Saint-Venant Kirchhoff material (left) and neo-Hookean material (right) (circular arch)

6.4 Example-IV (Torus subjected to compression)

In this numerical example, we consider a torus with inner radius $8m$ and outer radius $10m$ subjected to a vertical load $(0, 0, \pm 0.3)^T N/m^2$ along the diagonally opposite external edges in the plane $z = 0$ with a range of $P_x = 4.5m$ as shown in Figure 7. In addition to this, the torus is fixed in x-direction in

Table 3
Comparison of numerical results (circular arch using Saint-Venant Kirchhoff material law)

ν	Case I ($\alpha = 0$)	Case II	Case III	Q_1	Q_1-P_0
0.49000	-0.371	-0.373	-0.377	-0.352	-0.373
0.49900	-0.370	-0.372	-0.376	-0.263	-0.372
0.49990	-0.369	-0.372	-0.376	-0.101	-0.372
0.49999	-0.369	-0.372	-0.376	-0.056	-0.372

Table 4
Comparison of numerical results (circular arch using neo-Hookean material law)

ν	Case I ($\alpha = 0$)	Case III	Case IV ($\alpha = 0$)	Q_1	Q_1-P_0
0.49000	-0.417	-0.417	-0.417	-0.396	-0.416
0.49900	-0.416	-0.417	-0.415	-0.231	-0.415
0.49990	-0.416	-0.417	-0.415	-0.069	-0.415
0.49999	-0.416	-0.417	-0.415	-0.032	-0.415

the plane $x = 0$, in y-direction in the plane $y = 0$ and in z-direction in the plane $z = 0$. Geometrically nonlinear Saint-Venant Kirchhoff material is considered with Young's modulus $E = 17N/m^2$, and Poisson's ratio $\nu = 0.499$. The implementation is performed with six quasi-static steps. The deformed meshes obtained using Case II of the mixed formulation and the standard Q_1 formulation are shown in Figure 7. As expected the standard Q_1 formulation shows locking effect.

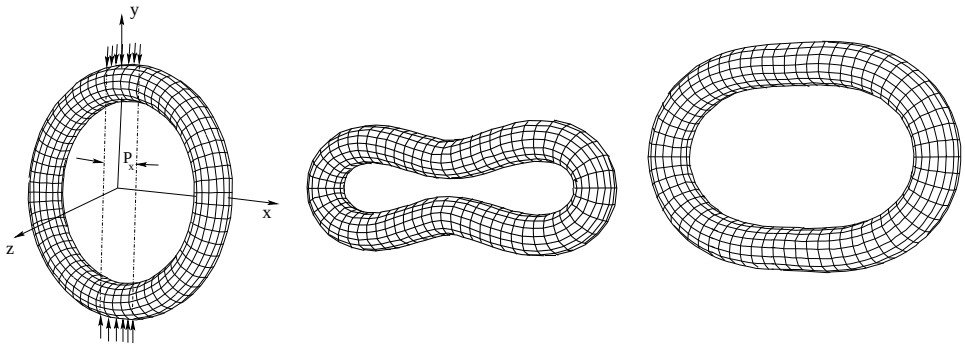

Fig. 7. Geometrical data (left), deformed shape with the mixed formulation Case-II (middle) and deformed shape with the standard Q_1 formulation (right) (torus under compression)

6.5 Example-V (Bending of a cylindrical shell)

In this example, the proposed three-field formulation is used to model a cylindrical shell pinched by a radial load along the outer edge, see also [28]. Taking advantage of the symmetry of the problem, only one quarter of the cylinder is modeled. In addition to the symmetric boundary conditions, the external lower edge of the cylinder is fixed in y-direction. The load is applied as a uniformly distributed force on the upper longitudinal section. The geometrical dimensions and material data used are given in Table 5.

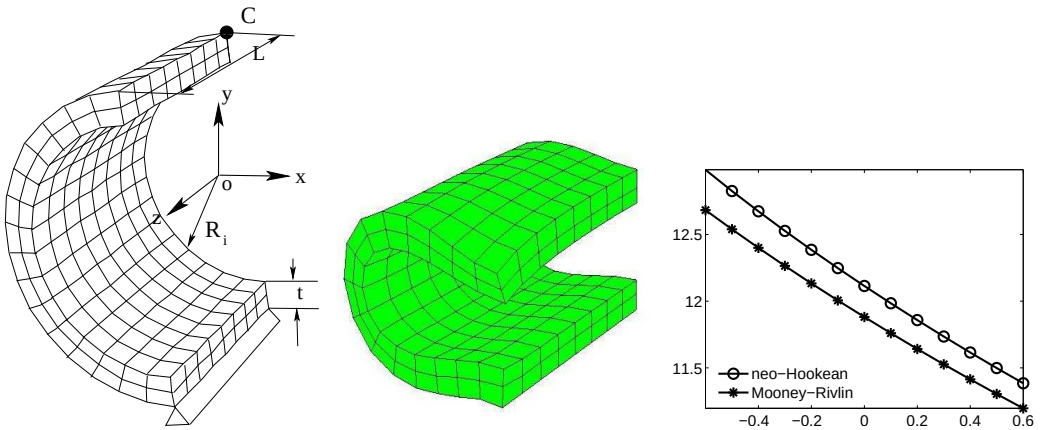

Fig. 8. Problem setting (left), deformed configuration (middle) and y-displacement at C versus $\frac{\alpha}{2}$ (right) (cylindrical shell)

Table 5
Geometrical and material data (cylindrical shell)

E	17853.6585 N/mm^2
ν	0.4878
t	$2mm$
R_i	$9mm - t/2$
L	$15mm$
c_m	0.2

Finite element analysis is performed using 24 quasi-static steps with an equal load increment in each step resulting in a total load of $P_0 = 450N/mm^2$. The study of convergence has been performed with a shell thickness of $2mm$.

The numerical solution at C along the y-direction using neo-Hookean material law are given in Tables 6 and 7 for Cases I ($\alpha = 0$) and III, respectively, whereas numerical results with Cases I ($\alpha = 0$) and III with Mooney–Rivlin material model ($c_m = 0.2$) using different finite element meshes are presented in Tables 8 and 9, respectively. The load factor γ_p is defined as $\gamma_p = P/P_0$

with the applied load P. As in other examples, we can observe a good convergence behavior for both material laws with both cases. We note that the difference between Mooney–Rivlin and neo-Hookean material laws depends on the material property. In the right picture of Figure 8, we show the absolute value of the y-displacement at C with respect to $\alpha/2$ using the space of stress from Case I for neo-Hookean and Mooney–Rivlin material laws with the mesh $16 \times 8 \times 2$. As in our other examples, the locking effect is more dominant for larger α.

In all our numerical results, we get the locking-free response in the nearly incompressible limit from all cases of our mixed formulations. In particular, the space of stress from Case I shows better behavior in almost all considered examples. However, more numerical experiments are necessary to test the performance of our α-dependent mixed formulation for the general hyperelastic model.

Table 6
Convergence of numerical results with Case I (neo-Hookean material law)

Mesh Load factor γ_p	$8 \times 4 \times 2$	$12 \times 6 \times 2$	$16 \times 8 \times 2$	$20 \times 10 \times 2$	$24 \times 12 \times 2$
0.1667	-1.2193	-1.402	-1.470	-1.502	-1.521
0.3333	-2.6437	-3.066	-3.230	-3.311	-3.357
0.5000	-4.2480	-4.974	-5.272	-5.423	-5.510
0.6667	-5.9512	-7.046	-7.519	-7.765	-7.909
0.8333	-7.6452	-9.167	-9.852	-10.218	-10.435
1.0000	-9.2555	-11.252	-12.114	-12.698	-13.004

Table 7
Convergence of numerical results with Case III (neo-Hookean material law)

Mesh Load factor γ_p	$8 \times 4 \times 2$	$12 \times 6 \times 2$	$16 \times 8 \times 2$	$20 \times 10 \times 2$	$24 \times 12 \times 2$
0.1667	-0.8396	-1.158	-1.342	-1.450	-1.517
0.3333	-1.7649	-2.497	-2.933	-3.193	-3.356
0.5000	-2.7872	-4.026	-4.782	-5.238	-5.523
0.6667	-3.9204	-5.732	-6.859	-7.534	-7.952
0.8333	-5.1755	-7.584	-9.091	-9.977	-10.521
1.0000	-6.5520	-9.535	-11.392	-12.474	-13.141

Table 8
Convergence of numerical results with Case I (Mooney-Rivlin material law)

Mesh Load factor γ_p	$8 \times 4 \times 2$	$12 \times 6 \times 2$	$16 \times 8 \times 2$	$20 \times 10 \times 2$	$24 \times 12 \times 2$
0.1667	-1.2318	-1.409	-1.476	-1.509	-1.527
0.3333	-2.6285	-3.040	-3.201	-3.281	-3.327
0.5000	-4.1948	-4.906	-5.197	-5.345	-5.431
0.6667	-5.8555	-6.931	-7.392	-7.634	-7.776
0.8333	-7.5121	-9.005	-9.673	-10.031	-10.243
1.0000	-9.0944	-11.044	-11.881	-12.450	-12.749

Table 9
Convergence of numerical results with Case III (Mooney-Rivlin material law)

Mesh Load factor γ_p	$8 \times 4 \times 2$	$12 \times 6 \times 2$	$16 \times 8 \times 2$	$20 \times 10 \times 2$	$24 \times 12 \times 2$
0.1667	-0.8710	-1.189	-1.374	-1.482	-1.549
0.3333	-1.7959	-2.529	-2.965	-3.225	-3.388
0.5000	-2.8172	-4.056	-4.813	-5.269	-5.555
0.6667	-3.9484	-5.760	-6.889	-7.565	-7.985
0.8333	-5.2002	-7.609	-9.118	-10.006	-10.553
1.0000	-6.5717	-9.555	-11.413	-12.498	-13.164

References

[1] J. Simo, M. Rifai, A class of assumed strain methods and the method of incompatible modes, International Journal for Numerical Methods in Engineering 29 (1990) 1595–1638.

[2] J. Simo, F. Armero, Geometrically nonlinear enhanced strain mixed methods and the method of incompatible modes, International Journal for Numerical Methods in Engineering 33 (1992) 1413–1449.

[3] S. Glaser, F. Armero, On the formulation of enhanced strain finite elements in finite deformation, Engineering Compuations 14 (1997) 759–791.

[4] F. Armero, On the locking and stability of finite elements in finite deformation plane strain problems, Computers and Structures 75 (2000) 261–290.

[5] D. Braess, C. Carstensen, B. Reddy, Uniform convergence and a posteriori error estimators for the enhanced strain finite element method, Numerische Mathematik 96 (2004) 461–479.

[6] T. Pian, K. Sumihara, Rational approach for assumed stress finite elements, International Journal for Numerical Methods in Engineering 20 (1984) 1685–1695.

[7] U. Andelfinger, E. Ramm, EAS-elements for two-dimensional, three-dimensional, plate and shell structures and their equivalence to HR-elements, International Journal for Numerical Methods in Engineering 36 (1993) 1311–1337.

[8] H. Hu, On some variational principles in the theory of elasticity and the theory of plasticity, Scientia Sinica 4 (1955) 33–54.

[9] K. Washizu, Variational methods in elasticity and plasticity, 3rd Edition, Pergamon Press, 1982.

[10] E. Kasper, R. Taylor, A mixed-enhanced strain method. Part I: geometrically linear problems, Computers and Structures 75 (2000) 237–250.

[11] E. Kasper, R. Taylor, A mixed-enhanced strain method. Part II: geometrically nonlinear problems, Computers and Structures 75 (2000) 251–260.

[12] G. Romano, F. Marrotti de Sciarra, M. Diaco, Well-posedness and numerical performances of the strain gap method, International Journal for Numerical Methods in Engineering 51 (2001) 103–126.

[13] B. Lamichhane, B. Reddy, B. Wohlmuth, Convergence in the incompressible limit of finite element approximations based on the Hu-Washizu formulation, Numerische Mathematik 104 (2006) 151–175.

[14] S. Brenner, L. Sung, Linear finite element methods for planar linear elasticity, Mathematics of Computation 59 (1992) 321–338.

[15] M. Vogelius, An analysis of the p-version of the finite element method for nearly incompressible materials. Uniformly valid, optimal error estimates, Numerische Mathematik 41 (1983) 39–53.

[16] J. Djoko, B. Lamichhane, B. Reddy, B. Wohlmuth, Conditions for equivalence between the Hu-Washizu and related formulations, and computational behavior in the incompressible limit, Computer Methods in Applied Mechanics and Engineering 195 (2006) 4161–4178.

[17] V. Girault, P.-A. Raviart, Finite Element Methods for Navier-Stokes Equations, Springer-Verlag, Berlin, 1986.

[18] R. Adams, Sobolev Spaces, Academic Press New York, 1975.

[19] H. Stolarski, T. Belytschko, Limitation principles for mixed finite elements based on the Hu-Washizu variational formulation, Computer Methods in Applied Mechanics and Engineering 60 (1987) 195–216.

[20] E. Stein, M. Rüter, Finite element methods for elasticity with error-controlled discretization and model adaptivity, in: E. Stein, R. de Borst, T. Hughes (Eds.), Encyclopedia of Computational Mechanics, Wiley, 2004, pp. 5–58.

[21] J. Nagtegaal, D. Parks, J. Rice, On numerically accurate finite element solutions in the fully plastic range, Computer Methods in Applied Mechanics and Engineering 4 (1974) 153–177.

[22] J. Simo, R. Taylor, K. Pister, Variational and projection methods for the volume constraint in finite deformation elasto-plasticity, Computer Methods in Applied Mechanics and Engineering 51 (1985) 177–208.

[23] D. Braess, P.-B. Ming, A finite element method for nearly incompressible elasticity problems, Mathematics of Computation 74 (2005) 25–52.

[24] P. Ciarlet, Mathematical Elasticity Volume I: Three-Dimensional Elasticity, North-Holland, Amsterdam, 1988.

[25] S. Timoshenko, J. Goodier, Theory of Elasticity, 3rd Edition, McGraw-Hill, New York, 1970.

[26] D. Mijuca, On hexahedral finite element HC8/27 in elasticity, Computational Mechanics 33 (2004) 466–480.

[27] M. Küssner, B. Reddy, The equivalent parallelogram and parallelepiped, and their application to stabilized finite elements in two and three dimensions, Computer Methods in Applied Mechanics and Engineering 190 (2001) 1967–1983.

[28] T. Merlini, M. Morandini, The helicoidal modeling in computational finite elasticity. Part III: Finite element approximation for non-polar media, International Journal of Solids and Structures 42 (2005) 6475–6513.